CARS2011

Section: CARS

ID: 0347

Abstract Title:
Automatic mask generation for 2D/3D image registration with clinical images of the pelvis

Authors:

Neuner M.[1], Steininger P. [1], Mittendorfer C. [2], Sedlmayer F. [1,2], Deutschmann H. [1,2]

[1]Paracelsus Medical University (PMU), Research and Development on Advanced Radiation Technologies (radART), Salzburg

[2]Landeskrankenhaus Salzburg (SALK), Universitätsklinik für Radiotherapie und Radio-Onkologie, Salzburg

Abstract Text:
Purpose

The spatial alignment of pre- and intra-interventional data plays an important role in image-guided radiotherapy (IGRT). For instance, image-guided setup is performed, where prior to each treatment fraction the patient's anatomy is imaged and compared to the planned reference setup. The goal is to correct for day-to-day variations of the target location in the body and/or the patient on the couch, in order to guarantee an efficient treatment and to avoid adverse effects.
Currently, in our institution two X-rays from different directions are acquired to verify and manually adjust the target position based on projected 3D structures (e.g. skeleton, gold-seeds). In the future a (semi-)automatic intensity-based 2D/3D registration approach will be employed to correct translational and rotational displacements in the pelvic region.
Intensity based 2D/3D registration requires similarity measures (metrics) to find the “optimal” spatial transformation between two or more datasets by employing iterative optimization over the search space, defined by the parameters of the transform. The metric measures how well the fixed image(s) (e.g. X-rays) fit the respective transformed moving image(s) (e.g. digitally reconstructed radiographs - DRRs - of the planning CT).
In general, metrics must cope with dissimilarities between the investigated images. Such discrepancies may be due to differing imaging modalities, acquisition times, occlusions emerging from body parts or additional objects (e.g. patient positioning aids) and shifts of soft tissue and/or bones.
In order to restrict the registration to the structures/anatomy of interest, the pixels used for metric evaluation must be constrained with a fixed image mask (e.g exclude femurs when registering on the bony anatomy of the pelvis).
To limit the metric evaluation to the anatomical structure of interest, we implemented an automated approach to construct a fixed image mask of the pelvis. We further validate the influence of four different mask shapes in combination with four different metrics and perform 2D/3D registration of planning CTs with two X-ray images from 27 fractions of six patients.

Methods

To validate the mask generation pipeline 27 fractions (out of 181) were randomly sampled from six patients. Per fraction two X-ray images (410×410mm, spacing resampled to 1×1mm from 0.4×0.4mm), taken from different views (gantry angles 154/244, 26/296, 135/225, 45/315, 180/270, 90/180°), were pre-processed with unsharp masking and used as registration input, along with the corresponding six planning CTs (pelvic region, spacing 0.977×0.977×2.5mm).
Four different fixed image masks were used: centered rectangular mask with a fixed size of 300×260mm (M1), centered rectangular mask that excludes the femurs (where possible) with a fixed height of 220mm (M2), automatic generated mask (M3) and a smoothed automatic generated mask (M4) as described below.
The masks M3/M4 were generated from an existing 3D structure of bony anatomy and the planning target volume (PTV). The pelvis and femurs were extracted by clipping the triangulated skeletal structure with boxes, based on the skeleton measurements and the PTV location. The resulting pelvis structure was dilated by moving the vertices 10mm in the direction of the point-normals, and the femur structures were dilated by 2mm (see figure 1). The dilated pelvis structure was limited to exclude regions close to the CT boundaries. The dilated structures were projected onto the X-ray plane of each view by using the known projection geometry of a Elekta Synergy linear accelerator (LINAC). The 2D binary masks of the femurs were subtracted from the 2D pelvis mask. Finally, the result was

further processed by a curvature constrained front propagation (hole/cavity filling, island removal), which uses a quorum (voting) algorithm.
Four different metrics were used: normalized cross correlation (NCC, sample mean is subtracted from sample values), stochastic rank correlation (SRC, fixed image histogram: 128 bins, range [0,255]; moving image histogram: 128 bins, range [DRR_{min},1.05*DRR_{max}]; 50% sample coverage), normalized mutual information (NMI, same histogram configuration as SRC) and gradient difference (GD).
AMOEBA (Nelder-Mead) optimization was used (maximum iterations 300, parameter tolerance 0.1, cost function tolerance 0.5, initial simplex delta 1, parameter scales weight 1° rotation equally to 1mm translation). DRR computation was performed with a fast ray-casting algorithm based on OpenGL. All computations were performed on a desktop computer (4×2.4GHz CPUs, 8MB L2-cache, 1066MHz FSB, 8GB RAM, 512MB GPU nVIDIA GeForce 9800GTX+, 7200rpm HDD) with 64bit i686 Linux as operating system.
The metric and optimizer configuration was kept constant for all 432 performed registrations, but could be further optimized. The final transformation of the 2D/3D registration was compared to a reference, which is the result of a translational, manual registration by a medical expert. The target registration error (TRE) related to the treatment plan isocenter was used as error measure. Only laser guided, skin-tattoo-based patient positioning was performed, with no further manual registration initialization. The registration was automatically initialized by a normalized correlation based search (rectangular radius 30mm) of a 80×80mm region around the projected skeletal structure center. The mean initial TRE to the planned location (isocenter) was 6.94mm with range [2.43,13.61mm].

Results

The registration results of the 432 registrations are summarized in table 1. NCC performed most stable (M2-4) with all masks and had the lowest mean (<1,69mm M2-4) and maximum TRE (<3.47 M2-4) of all metrics. M2 showed the same performance as M3 and M4 with NCC. All other metrics had lower errors with M3/M4, compared to M1/M2, where SRC profited most (mean TRE 2.04 vs. 1.82mm, max. TRE 6.1 vs. 4.87mm). NCC and SRC performed worst at M1 and better with additional masking. In contrast NMI and GD show similar performance with M1, M3 and M4. GD had problems with M2 (max. TRE 19.58mm).
The automatic correlation based registration initialization computation time was 1.49s on average (n=432) with range [1.13,3.69s]. The M3 and M4 mask generation took 3.06 and 3.62s on average (n=108). The mean registration times range from 7.43 to 19.94s (n=27) with single registration times in range [4.16,45.29s] (n=432). The registration required 70.26 to 147.52 iterations on average (n=27).

Conclusion

Constraining the metric evaluation to the desired features had advantageous effects on the registration performance (see table 1). GD had some stability problems (max. TRE) at the M2 mask. SRC performed better with the automatic generated masks. Though, the computed TRE is biased because the reference transformation only considers translations and no rotations. In terms of computation time SRC and NMI performed best, while NCC showed the lowest registration error.
The 10mm dilation of the 3D pelvis structure may limit the capture range, because at large initial translations important structures can lie outside of the mask. The computation times with M3/M4 were longer, due to the mask generation step, but should decrease the errors if more influential structures are excluded from the registration (e.g. tools, positioning aids at head and neck treatments).
Summing up, we are confident that this mask generation approach improves the 2D/3D image registration performance with real clinical images.

Figure 1: Pipeline of automatic pelvis mask generation (top) and examples of the used fixed image masks (magenta=M1, blue=M2, red=M3, green=M4, yellow=M3/M4). Shown are the unsharp masked views 135/225, 154/244, 90/180° of three different patients.

Table 1: Summary of the 2D/3D target registration errors (TRE) with standard error ($SE=\sigma*n^{-0.5}$), minimum (Min), median (P50), 95th percentile (P95) and maximum (Max) for n=27 fractions. Furthermore, the mean registration times and average number of iterations are provided.

fig.1

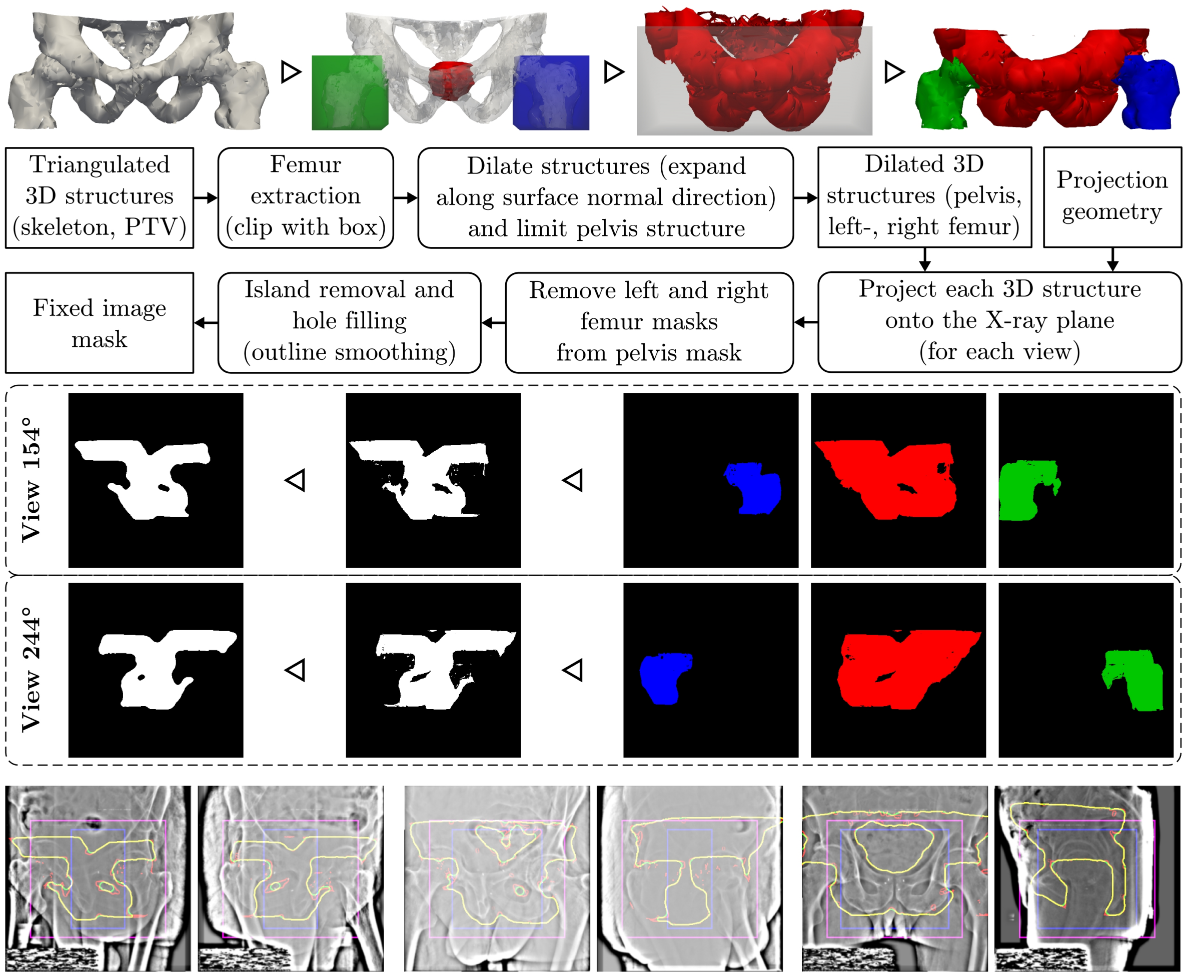
Triangulated 3D structures (skeleton, PTV)
Femur extraction (clip with box)
Dilate structures (expand along surface normal direction) and limit pelvis structure
Dilated 3D structures (pelvis, left-, right femur)
Projection geometry
Project each 3D structure onto the X-ray plane (for each view)
Remove left and right femur masks from pelvis mask
Island removal and hole filling (outline smoothing)
Fixed image mask
View 154°
View 244°

fig.2

Metric	Mask	TRE						Time	Iterations
		Mean [mm]	±SE	Min [mm]	P50 [mm]	P95 [mm]	Max [mm]	Mean [s]	Mean
NCC	M1	2.37	±0.43	0.37	1.37	7.51	8.68	13.10	125.93
NCC	M2	1.61	±0.16	0.37	1.32	3.09	3.15	11.53	119.52
NCC	M3	1.63	±0.16	0.58	1.60	3.13	3.25	12.04	122.78
NCC	M4	1.69	±0.16	0.37	1.64	3.17	3.47	12.18	125.74
SRC	M1	2.43	±0.48	0.61	1.70	6.84	12.49	8.90	91.48
SRC	M2	2.04	±0.25	0.60	1.84	4.65	6.10	7.45	83.07
SRC	M3	1.79	±0.18	0.76	1.50	3.15	4.81	8.68	99.67
SRC	M4	1.82	±0.18	0.62	1.86	2.91	4.87	8.88	101.85
NMI	M1	2.36	±0.28	0.49	2.03	5.50	5.83	8.29	70.26
NMI	M2	2.24	±0.29	0.45	2.04	5.36	5.89	7.43	70.63
NMI	M3	2.10	±0.25	0.29	1.77	4.80	5.01	8.00	75.33
NMI	M4	2.04	±0.26	0.26	1.72	4.86	4.93	7.79	74.19
GD	M1	1.89	±0.19	0.67	1.83	3.78	4.69	19.23	138.48
GD	M2	2.91	±0.78	0.55	1.75	10.39	19.58	18.25	132.59
GD	M3	1.71	±0.18	0.49	1.56	3.58	3.90	19.66	147.52
GD	M4	1.86	±0.22	0.51	1.66	4.17	5.18	19.94	145.22